

Course 12.812, General Circulation of the Earth's Atmosphere
 Prof. Peter Stone
Section 4: Water Vapor Budget

Water Vapor Distribution

First let us look at the distribution of specific humidity, q . The seasonal mean distributions of $[\bar{q}]$ in g/kg, are given in Figure 12.4a of Peixoto and Oort (1992). We note:

- 1) $\rho_{\text{H}_2\text{O}} / \rho_{\text{air}}$, i.e., the mass mixing ratio, ranges from $\sim 10^{-2}$ in low latitudes near the ground to $\sim 10^{-3}$ at high latitudes or high altitudes.
- 2) The distribution closely resembles that of $[\bar{T}]$, because q is strongly controlled by the Clausius-Clapeyron Equation:

$$q < q(\text{saturated}) = q_s = \frac{\epsilon e_0}{p} \exp \left\{ -\frac{m_{\text{H}_2\text{O}} L_v}{R} \left(\frac{1}{T} - \frac{1}{T_0} \right) \right\}; \quad \text{where}$$

$$\epsilon = \frac{m_{\text{H}_2\text{O}}}{m_{\text{air}}} = \text{ratio of molecular weights} = 0.621,$$

$$e_0 = \text{saturated water vapor pressure at } T_0, \\ (= 6.11 \text{ mb if } T_0 = 273^\circ),$$

$$\frac{m_{\text{H}_2\text{O}} L_v}{R} = 5420 \text{ }^\circ\text{K}.$$

Therefore, for example, if we let $T = \bar{T} + T'$, and assume $T' \ll \bar{T}$, and choose $\bar{T} =$ mean surface temperature = 288 °K, then

$$q_s = \frac{\text{const}}{p} e^{.065 T'};$$

\therefore a T' of $\pm 11^\circ\text{C} \Rightarrow$ a doubling or halving of q_s , and the temperature variations are much more important than p variations. This constrains q to fall off rapidly with height and latitude.

- 3) The scale height of q is $\sim 250 \text{ mb} \sim 2.5 \text{ km}$ near the ground. E.g., if $T' = -\Gamma z$ with $\Gamma = 5^\circ / \text{km} \cong$ mean lapse rate of lower troposphere, then

$$q_s = \frac{\text{const}}{p} e^{-z/H}, \quad H = \frac{1}{.065\Gamma} = \frac{1}{.065 \times 5} = 3.1 \text{ km}.$$

q falls off more rapidly than q_s , because the relative humidity ($r = q/q_s$) decreases with height. (See Figures 16 and 17 in Lorenz (1967)). It is near 80% at the surface and near 40% at 500 mb. However, the q_s change with height dominates the change in q .

More generally, looking at these same figures, we note

- 1) $r \lesssim 1$.
- 2) seasonal changes in r are \ll changes in q , because of the Clausius-Clapeyron equation. (Simple climate models often approximate $r = \text{constant}$.)
- 3) r is a minimum in the subtropics.

The seasonal changes are illustrated in Figure 12.4a of Peixoto and Oort (1992). The seasonal changes are a maximum in mid and high latitudes, because the T changes are largest there, and are a maximum near the ground, since the moisture content is a maximum there. The maximum seasonal excursions are $\sim \pm 3$ g / kg -- e.g., at 40N, 1000 mb; q ranges from ~ 5 g / kg in January to ~ 11 g / kg in July.

Peixoto and Oort (1983) have looked at longitudinal variations in \bar{q} . The longitudinal variations are smaller than the latitudinal variations ($\sim 1/3$ as large) so \bar{q} does tend to be zonal. The zonal variations are primarily associated with the deserts. The largest anomaly is over the Sahara, where q is about 60% of the mean zonal value at the same latitudes ($q^*_{\min} \cong 0.6[\bar{q}]$).

Equations and Definitions

Let ρ = density of air, q = specific humidity (grams of water vapor per kilogram of air). Then the conservation law for water vapor is

$$\boxed{\frac{\partial}{\partial t}(\rho q) + \nabla \cdot \rho q \bar{v} = -C + F_q},$$

where $F_q = \nabla \cdot \rho D \nabla q \cong \frac{\partial}{\partial z}(\rho D \frac{\partial q}{\partial z})$.

F_q represents molecular diffusion, and C = the net local condensation rate per unit volume, i.e., condensation minus evaporation. Because of mass conservation,

$$\frac{\partial \rho}{\partial t} + \nabla \cdot (\rho \bar{v}) = 0,$$

we can rewrite the conservation equation as

$$\frac{\partial q}{\partial t} + \vec{v} \cdot \nabla q = \frac{dq}{dt} = -\frac{C}{\rho} + \frac{F_q}{\rho};$$

now it is convenient to use pressure coordinates:

$$\text{since } \frac{\partial u}{\partial x} + \frac{\partial v}{\partial y} + \frac{\partial \omega}{\partial p} = 0,$$

$$\text{we have } \frac{\partial q}{\partial t} + \frac{\partial}{\partial x}(uq) + \frac{\partial}{\partial y}(vq) + \frac{\partial}{\partial p}(\omega q) = -\frac{C}{\rho} + \frac{F_q}{\rho}.$$

Now we consider the balance averaged over t:

$$\frac{\overline{\partial q}}{\partial t} = \frac{q(T) - q(0)}{T}.$$

We can neglect this for an annual mean because of periodicity (neglecting climate change, $q(T) = q(0)$) or for a seasonal extreme, where by definition $\frac{\partial q}{\partial t} = 0$. For other situations we can neglect this term if, for example, it is small compared to the advective term, e.g., the meridional flux term:

$$\frac{\partial}{\partial y}(\overline{vq}) \sim \frac{|v| |q|}{L_y};$$

(N.B., the eddy flux dominates the total transport.) Taking $v \sim 10$ m/s, $L_y \sim 3000$ km, we can neglect $\partial q / \partial t$ if $T \gg \frac{L_y}{v} \sim \frac{3000 \text{ km}}{10 \text{ m/s}} \sim 3 \times 10^5 \text{ sec} \sim 4 \text{ days}$. E.g., even for an equinox monthly average it can be neglected as a first approximation.

If we now also average zonally and apply the condition of periodicity, and integrate vertically from $[\bar{p}] = p_s$ to $p = 0$, and apply the boundary condition that $\omega = 0$ on $p = 0$, we obtain:

$$\left[\int_0^{p_s} \frac{\partial}{\partial y}(\overline{vq}) dp \right] - [\omega_s q_s] = - \left[\int_0^{p_s} \left(\frac{\bar{C}}{\rho} - \frac{\bar{F}_q}{\rho} \right) dp \right].$$

We further approximate that the storage of water in liquid or solid form in a unit column is very small compared to the rate of precipitation, P, or evaporation, E, at the surface per unit area. Typical values for the storage of water in a column of the atmosphere are ~ 0.2 g/cm² which equals ~ 0.2 cm of precipitable water. For comparison, typical values of P and E are ~ 100 cm/yr ~ 0.3 cm/day. Thus atmospheric storage can be neglected for

averaging periods long compared to one day. We also neglect the time mean horizontal variations of p_s ($\sim 3\%$ error). If we invoke hydrostatic equilibrium, we can integrate the diffusion term:

$$\int_0^{p_s} \frac{\overline{F}_q}{\rho} dp = g \int_{p_s}^0 \overline{F}_q dz = -gE.$$

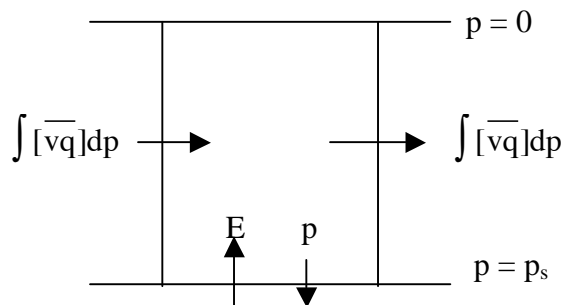
And by definition, if water storage in the atmosphere is negligible, then the net condensation term when integrated just gives us the precipitation:

$$\int_0^{p_s} \frac{C}{\rho} dp = -g \int_{\infty}^{\text{surface}} C dz = gP.$$

Therefore our balance equation reduces to

$$\frac{\partial}{\partial y} \int_0^{p_s} [\overline{vq}] dp = g[\overline{E} - \overline{P}].$$

This states that the net divergence of water vapor from a unit column must be balanced by a net excess of evaporation over precipitation at the surface as illustrated in the diagram.



It is valid for annual mean states, seasonal extremes, and other averaging periods $T \gg 4$ days, i.e., $T \gtrsim 1$ month.

Annual Balance in Latitude belts

(i) Transports

First we look at the transports. Using our earlier formalism, we can break $[\overline{vq}]$ into 3 contributions:

$$[\overline{vq}] = [\overline{v}][\overline{q}] + [\overline{v'q'}] + [\overline{v'q'}]$$

$$\text{total} = \text{MMC} + \text{SE} + \text{TE}$$

Peixoto and Oort (1983) give the vertically averaged contributions to $[\overline{vq}]$ calculated from 5/63 – 4/73 (10 years). The integration was from 1000 to 250 mb, and the analysis was for 7-levels: 1000, 950, 900, 850, 700, 500, and 300 mb. (The vertical distributions are trivial – they all peak in the lowest 100 mb of the atmosphere, near the top of the planetary boundary layer, and fall off rapidly above that because of the Clausius-Clapeyron equation.) The following table gives Peixoto and Oort's results for the

mean $[\overline{vq}]$, i.e., $\frac{1}{p_s} \int_0^{p_s} [\overline{vq}] dp$, in (m/sec) (g/kg) – i.e., multiply by 10^{-1} to get cgs units.

Annual Mean Moisture Fluxes in Atmosphere

Units: (m/sec) (g/kg)

	10S	0	10N	20N	30N	40N	50N	60N	70N
$[\overline{v}][\overline{q}]$	1.9	.8	-2.0	-1.1	.4	.4	.3	0	-.1
$[\overline{v'q'}]$	-.1	-.1	0	.4	.3	.1	.1	.1	0
$[\overline{v'q'}]$	-.5	0	.5	.8	1.3	1.5	1.3	.9	.5
total	1.3	.8	-1.5	0	2.0	2.0	1.7	1.0	.4

We see that the MMC dominates in low latitudes, TE's dominate in high latitudes, and SE's only give a minor contribution. The directions of the MMC and TE transports are easy to understand. Since q is concentrated near the ground, the MMC transports are dominated by the lower branches of the cells, and we have an equatorward transport by the Hadley cells, a much smaller poleward transport by the Ferrel cell, and an even smaller equatorward transport by the polar cell. The transient eddies are generally associated with warm air moving poleward and cold air moving equatorward. Since the warm air tends to be more moist (the Clausius-Clapeyron relation), the TE's have a net poleward transport of moisture.

To look at the balance, we have to compute the divergence of the above fluxes, which in spherical coordinates are equal to

$$\frac{1}{\cos \phi \Delta y} \left[\cos \phi \int_0^p [\overline{vq}] dp \right]_{\phi - \frac{1}{2} \Delta \phi}^{\phi + \frac{1}{2} \Delta \phi}$$

where Δy is the distance corresponding to $\Delta \phi$, $\Delta y = a \Delta \phi$. If we divide by g and express in cm/year, then we can compare directly with $[\overline{E} - \overline{P}]$ in cm/year. This comparison has been done by Peixoto (1972). However, he only computed $[\overline{vq}]$ from data from one year (1958,

the IGY) from about 450 stations (mostly in the Northern Hemisphere), and mostly from 4 pressure levels (1000, 850, 700, and 500 mb – note, this is not bad for q statistics). Thus we will supplement his values for the divergence of $[\overline{vq}]$ with the divergence calculated from Peixoto and Oort's 1983 data set, which is much more complete.

(ii) Precipitation

The \overline{P} and \overline{E} figures we will take from Baumgartner and Reichel (1976), which is a synthesis of many different analyses. In general the precipitation data is from historical data, and is subject to one great uncertainty: good P data over the oceans are lacking. Ocean precipitation rates are taken primarily from coastal and island observing stations. Analyses of precipitation measurements from ships show substantial local differences: for example, in the north Atlantic, where there are many ship observations, rates ~ 30% less have been found. Of course errors in zonal averages will be much less. A possible source of error in the ocean precipitation rates is that there may be systematic differences in rainfall over land and ocean – e.g., it may be greater over land because of the stronger diurnal heating. Thus coastal and island precipitation rates may not be typical of the oceans. Another source of error is the high degree of local variability in precipitation rates: rates measured show very little correlation when the station separation is $\gtrsim 100$ km. Therefore even over land measured precipitation rates may not give good mean values characteristic of area averages.

There have been more modern attempts to create precipitation climatologies. However they are also problematic. In the case of re-analyses, so far precipitation is not one of the assimilated data fields, so the precipitation is determined by the model. Thus the analysis at any given time has precipitation produced by the model in its forecast from the previous analysis time, usually 6 hours earlier. The model's precipitation is dependent on sub-grid scale parameterizations which are very uncertain. That they are problematic is seen in Figure 2 in Andersson et al. (2005). The analyzed P (at $t = 0$) is too large, as one can tell from Figure 2a which shows that one day later the tropical atmosphere has too low a relative humidity. As the forecast continues the precipitation decreases (Figure 2c), but the relative humidity does not improve (Figure 2b). Thus the precipitation rates are not acceptable. Note that the excess precipitation in the analysis gives a Hadley cell 1 day later (Figure 2d) which is stronger than the analysis, another indication that the analysis P is too strong.

Because of the problems with the re-analyses, another approach has been taken, i.e., using satellite data to infer precipitation. (See Adler et al. 2003). Primarily microwave and infra-red emissions are used, but the algorithms that are used to convert this data to precipitation must be calibrated against ground-based radar and rain-gauge measurements. The main advantage of this approach is that it gives continuous global coverage. This approach has been used by the Global Precipitation Climatology Project (GPCP) to produce monthly mean precipitation data on a $2\frac{1}{2} \times 2\frac{1}{2}$ grid. Figure 14 in Adler et al. (2003) shows a comparison of the GPCP output with local rain-gauge

measurements. The large scatter tells us that at best this approach can only be used for long term means. But even then, there is still a bias as indicated.

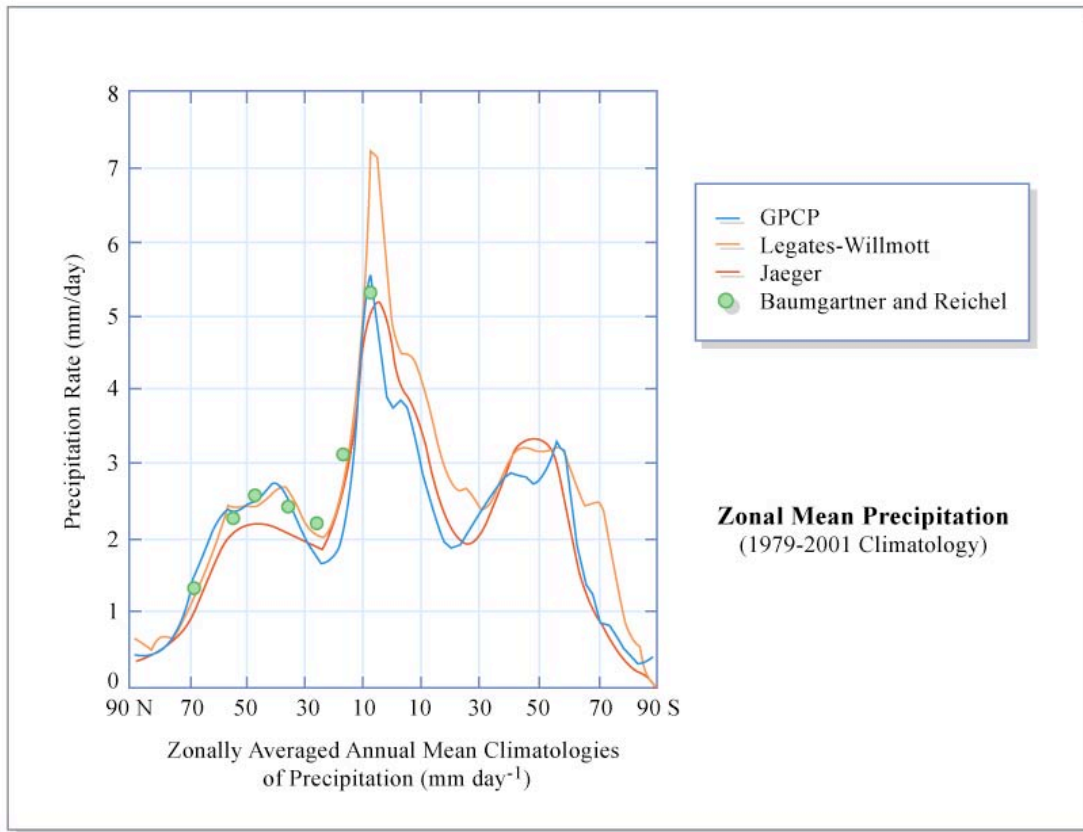


Figure by MIT OCW.

The above figure compares the GPCP product for annual mean zonal mean precipitation with earlier (ground-based) analyses like those used by Peixoto and Oort. We have superimposed the Baumgartner and Reichel (1975) Northern Hemisphere values on the Adler et al. plot. We see that there is no appreciable difference.

(iii) Evaporation

The situation with regard to E is even worse. Very few direct measurements of evaporation are available, and these are nowhere near sufficient for establishing climatological means. Therefore E must be calculated. Over land E is calculated as the residual between P and run-off. (Storage can be neglected for annual means.) Run-off is calculated from the volume of river and stream flows, etc, and has its own uncertainties. The method used over oceans is to calculate E locally from the formula

$$E = \rho c u (q_s - q) = \rho c u q_s (1 - r)$$

where ρ is the density of air, q_s is the saturation vapor pressure at the ocean temperature, and q and u are the observed (mean) humidity and wind speed at a standard level above the ground – e.g., 10 meters, or the level of ship observations. c is a phenomenological coefficient. In recent decades c has been determined from field experiments, by fitting the formula for E to actual measurements of E . This yields a mean value

$$c \cong 1.2 \times 10^{-3} \pm 10\%$$

The main source of error in calculating E from the formula is that c is not a constant – e.g., under calm conditions ($u \rightarrow 0$) c becomes very large, i.e., $E \neq 0$. When the formula is applied to climatological data, another source of error is the lack of good data for u . Variations in u occur on very small spatial and time scales and are generally not accurately measured. $[\bar{E}]$ errors, like those in $[\bar{P}]$, are probably $\sim 25\%$.

(iv) The Balance

The table below summarizes the values of \bar{P} , \bar{E} , and the dynamical flux divergences in cm/year for various latitude belts.

Annual Mean Moisture Balance in the Atmosphere
Unit: cm/year

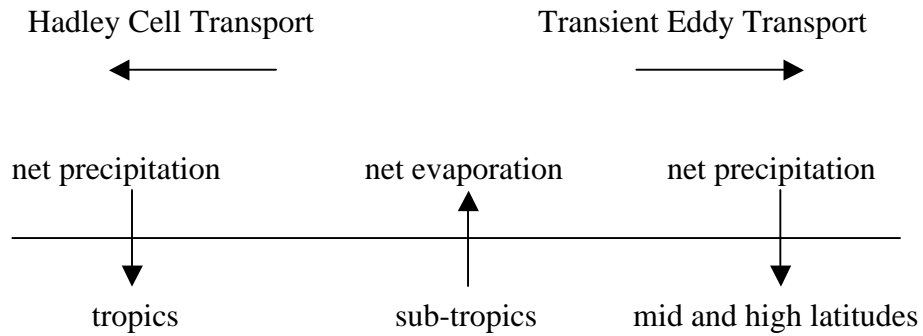
	0-10N	10-20N	20-30N	30-40N	40-50N	50-60N	60-70N
$[\bar{E}]^1$	125	128	111	97	64	45	28
$[\bar{P}]^1$	189	112	68	76	87	84	51
$[\bar{E} - \bar{P}]^1$	-64	16	43	21	-23	-39	-23
$\text{div } \bar{v}q^2$	-48	32	44	-2	-16	-25	-23
$\text{div } \bar{v}q^3$	-75	30	48	26	-27	-36	-19

Sources:

1. Baumgartner and Reichel, 1975,
2. Peixoto and Oort, 1983,
3. Peixoto, 1972.

In checking the balance, we see that there is another source of error: $E - P$ represents the difference between two noisy fields, and thus is even noisier. For example, if we take the errors in P and E to be 10%, and random, then between 30 and 40N the error in P is ± 10 , in $E \pm 8$, and in $[\bar{E} - \bar{P}] \pm 13$. Therefore the disagreement with $\text{div } \bar{v}q$ from Peixoto and Oort is only two times the probable error. In light of these errors the agreement with the dynamical divergences is satisfactory. In fact the estimate of $[\bar{E} - \bar{P}]$ obtained from the dynamical data is probably the most accurate one. The differences between Peixoto's earlier and Peixoto and Oort's later results are probably due to the small size of Peixoto's earlier data sample.

The above Table reveals the dominant features of the hydrological cycle, which can be diagrammed as follows:



The return flows below the surface necessary to complete the cycle are of course accomplished by rivers, ocean currents, and subterranean run-off. The dynamical transports explain why the relative humidity is a minimum in the subtropics (see Figures 16 and 17 in Lorenz (1967)).